MOLECULAR AND CELLULAR BIOLOGY, July 2007, p. 5201–5213 Vol. 27, No. 14
0270-7306/07/$08.00+0 doi:10.1128/MCB.02237-06

Transcriptional Repressor Erf Determines Extraembryonic Ectoderm Differentiation▽†

Chara Papadaki,[1] Maria Alexiou,[2] Grace Cecena,[3] Mihalis Verykokakis,[1] Aikaterini Bilitou,[1] James C. Cross,[4] Robert G. Oshima,[3] and George Mavrothalassitis[1]*

Medical School, University of Crete and IMBB, FORTH, Heraklion, Crete 710 03, Greece[1]; Institute of Immunology, BSRC Alexander Fleming, Vari 166 72, Greece[2]; The Burnham Institute for Medical Research, La Jolla, California 92037[3]; and Department of Biochemistry and Molecular Biology, University of Calgary, Calgary, AB T2N 4N1, Canada[4]

Received 29 November 2006/Returned for modification 13 February 2007/Accepted 2 May 2007

Extraembryonic ectoderm differentiation and chorioallantoic attachment are fibroblast growth factor (FGF)- and transforming growth factor β-regulated processes that are the first steps in the development of the placenta labyrinth and the establishment of the fetal-maternal circulation in the developing embryo. Only a small number of genes have been demonstrated to be important in trophoblast stem cell differentiation. *Erf* is a ubiquitously expressed Erk-regulated, ets domain transcriptional repressor expressed throughout embryonic development and adulthood. However, in the developing placenta, after 7.5 days postcoitum (dpc) its expression is restricted to the extraembryonic ectoderm, and its expression is restricted after 9.5 dpc in a subpopulation of labyrinth cells. Homozygous deletion of *Erf* in mice leads to a block of chorionic cell differentiation before chorioallantoic attachment, resulting in a persisting chorion layer, a persisting ectoplacental cone cavity, failure of chorioallantoic attachment, and absence of labyrinth. These defects result in embryo death by 10.5 dpc. Trophoblast stem cell lines derived from $Erf^{d11/d11}$ knockout blastocysts exhibit delayed differentiation and decreased expression of spongiotrophoblast markers, consistent with the persisting chorion layer, the expanded giant cell layer, and the diminished spongiotrophoblast layer observed in vivo. Our data suggest that attenuation of FGF/Erk signaling and consecutive Erf nuclear localization and function is required for extraembryonic ectoderm differentiation, ectoplacental cone cavity closure, and chorioallantoic attachment.

The *ets* gene family of transcription factors is characterized by the common winged-helix DNA binding domain and has been implicated in a wide range of processes, most commonly lymphoid differentiation and oncogenesis (for reviews see references 3, 29, 52, 55, and 57). The other common characteristic of the ets domain proteins is that they are regulated by extracellular signaling, mainly the receptor tyrosine kinase (RTK)/mitogen-activated protein kinase pathway (63, 65).

Erf is an ets domain transcriptional repressor (56) that is regulated by the *RTK/ras/erk* pathway via subcellular localization as a result of its specific interaction (45) and phosphorylation by Erk1/2 (36). It has been shown that it can suppress ets- and ras-induced transformation in fibroblasts (35), suggestive of its role within the RTK/ras signaling pathway. In the absence of Erk activity Erf is nuclear and can suppress fibroblast proliferation in a retinoblastoma-dependent manner, providing another link in RTK signaling and cell cycle. However, its in vivo function remains elusive.

The presence of multiple ets domain proteins in any cell at all times (27) and their ability to interact with similar DNA sequences as monomers hinders the effort to decipher the biological role of specific *ets* genes. However, recent gene-targeting approaches have been valuable in this regard. Homozygous deletion of three members of the *ets* family in mice, *GABPα* (50), *Ets2* (69), and *Elf5* (12), have been shown to affect early placenta development, while a fourth one, *TEL*, has been shown to affect yolk sac angiogenesis (67). Two more *ets* genes, *Pea3* and *Erm*, induce male sterility, making the reproductive process the most common target of this family of transcription factors (5, 34).

The inner cell mass and the trophoectoderm are the first two distinguishable cell layers during embryogenesis. Trophoectoderm cells give rise to the first organ formed in mammalian development, the placenta. Considerable insight has been gained in the last few years on the mechanisms and genes involved in cell fate determination during placenta development. The plethora of mutant mouse lines that exhibit placental defects is the primary reason for our increased understanding of placenta development. More than 100 genes have been shown to affect proper trophoblast stem cell (TSC) maintenance and differentiation to the cell types that constitute the placenta (for reviews see references 51 and 59).

TSC self-renewal and proliferation depends on fibroblast growth factor (FGF) and transforming growth factor β (TGFβ) family members, and these factors have been used successfully to derive TSCs from mouse blastocysts (2, 14, 15, 25, 62, 64). *Cdx2* is the first gene that determines trophoectoderm identity (41) and, together with *Eomes* (53), *Errβ* (40), and *Elf5* (12), is required for extraembryonic ectoderm (ExE) development. Trophoectoderm gives rise to the chorion, ectoplacental cone, and giant cell layers. The spongiotrophoblast layer arises from

* Corresponding author. Mailing address: Medical School, University of Crete, Voutes, Heraklion, Crete 710 03, Greece. Phone: 30-2810-394537. Fax: 30-2810-394530. E-mail: mavro@imbb.forth.gr.

† Supplemental material for this article may be found at http://mcb.asm.org/.

▽ Published ahead of print on 14 May 2007.

the ectoplacental cone and contributes to the giant cell layers, while the chorion gives rise to the labyrinth layer after the attachment with the embryo-derived allantois. *Cdx2*, *Eomes*, and *Err*β are also required for chorion development, while *Mash2* (23) and *Tpbpa* are required for proper ectoplacental cone development. *Tpbpa* is also required for spongiotrophoblast differentiation, while *Hand1* (17, 47) and *Stra13* can promote giant cell differentiation. In contrast to the other placenta layers, very little is known about the differentiation of chorionic cells to the cell types that contribute to making up the labyrinth. *Gcm1* is the only gene so far known to be required for differentiation of chorionic trophoblast cells to syncytiotrophoblasts (1). Chorioallantoic attachment occurs when the mesodermally derived allantois grows from the caudal region of the embryo across the exocoelomic cavity and makes contact with the chorionic mesothelium. This is a critical step required for labyrinth development. *VCAM-1* and *integrin* α*4* are important mediators of this process (24, 33, 70), while the TGFβ and the Wnt signaling pathways have also been implicated in chorioallantoic attachment (30, 44, 64).

In order to determine the *Erf* function in vivo, we generated transgenic mice carrying a homozygous mutation of the gene that eliminates *Erf* mRNA and protein production. These mice die in utero at day 10 due to severe placenta defects. $Erf^{dI1/dI1}$ embryos fail to undergo chorioallantoic attachment and labyrinth development and instead have an expanded chorion layer that fails to further differentiate. Interestingly, they also fail to close the ectoplacental cone cavity, suggesting that *Erf* may be the first gene identified that regulates this process. In addition, $Erf^{dI1/dI1}$ placentas have abnormalities in the giant cell and spongiotrophoblast layers. $Erf^{dI1/dI1}$ trophoblast stem cell lines have a delayed differentiation compared to wild-type TSCs and fail to express specific differentiation markers.

Our data indicate that Erf, as an effector in the FGF pathway, contributes to the proper differentiation of trophoblast stem cells and is required for the differentiation of chorionic trophoblasts, and they suggest that proper chorion differentiation is necessary for chorioallantoic attachment and ectoplacental cone cavity closure.

MATERIALS AND METHODS

Cell lines. PrmCre embryonic stem (ES) cells (42) were maintained on a monolayer of γ-irradiated neomycin-resistant primary embryonic fibroblasts in knockout Dulbecco's modified Eagle's medium (Invitrogen) supplemented with 15% fetal calf serum (FCS) (HyClone), 0.1 mM nonessential amino acids, 0.2 mM L-glutamine, 0.1 mM 2-mercaptoethanol, and 1,000 U/ml leukemia inhibitory factor (Chemicon).

TSCs from 3.5-days-postcoitum (dpc) blastocysts were derived and maintained in 70% mouse embryo fibroblast condition medium, 30% RPMI supplemented with 20% fetal calf serum, 25 ng/ml FGF4, and 1 μg/ml heparin as previously described (62). Differentiation was induced by plating 10^5 cells in 60-mm-diameter plates and replacing the medium 24 h later (day 0) with 85% RPMI, 15% FCS.

Targeting. A 7-kb NotI genomic *Erf* region covering exons 2 to 4 and the 3′ untranslated region (39) was used to construct the targeting vector. An 890-bp AvrII/BamHI fragment spanning exons 2, 3, and 100 bp from exon 4 was replaced with the 1.4-kb XbaI/SalI fragment of pL2neo vector (22) containing the neomycin resistance gene flanked by loxP sites. A 7.5-kb SalI fragment was inserted into the pBSTK9 vector (60), which contains two thymidine kinase genes of the herpes simplex virus flanking the point of insertion. The targeting vector was linearized and electroporated into 10^7 ES cells. Transfected ES cells were selected in 0.3 mg/ml G418 (GIBCO-BRL) and 2 μM ganciclovir, and 179 drug-resistant ES clones were isolated 7 days later and analyzed.

Generation of chimeric mice. Chimeric mice were generated by microinjection of two independent ES clones, no. 130 and no. 169, into 3.5-dpc C57BL/6 blastocysts and implantation into pseudopregnant CD1 foster females (26). Chimeric males with high levels of chimerism were mated to CBAxC57BL/6 and 129/Sv females to produce mice heterozygous for the *Erf* mutant allele (Erf^{dI1}). The PrmCre ES cells contained the Cre recombinase gene driven by the protamine, resulting in Cre-mediated deletion of the *neo* gene cassette in the germ line of male chimeras. $Erf^{dI1/+}$ mice were intercrossed to generate the homozygous $Erf^{dI1/dI1}$ mice. Both no. 130 and no. 169 ES clones gave rise to *Erf*-deficient animals that exhibited identical phenotypes. All mice were maintained in a specific-pathogen-free animal facility at the Institute of Molecular Biology and Biotechnology.

Timed pregnancies, dissections, and histological analysis. Heterozygous male and female mice ($Erf^{dI1/+}$) were bred to obtain wild-type ($Erf^{+/+}$), heterozygous ($Erf^{dI1/+}$), and homozygous ($Erf^{dI1/dI1}$) mutant mouse embryos. Pregnant females were sacrificed at different stages of development. Uteri were removed and immersed in phosphate-buffered saline (PBS). Placentas were dissected and fixed in 4% paraformaldehyde in PBS overnight at 4°C, while embryos or yolk sacs were kept for genotyping or further examination. For hematoxylin and eosin staining placentas were dehydrated, embedded in paraffin wax, and cut into 7-μm sections (31). Whole-mount staining of yolk sac with hematoxylin was performed using standard protocols. Placentas used for cryosections were fixed in 4% paraformaldehyde overnight at 4°C, incubated with 30% sucrose in PBS overnight, embedded in OCT (Tissue Tek), and snap-frozen in dry ice-cooled 2-methylbutane. Placentas were stored at −80°C. Sections of 7 μm were cut on a cryostat, adhered to superfrost slides, air dried, and stored at −80°C. Tissues were dissected under a Leica MZ12 stereoscope, photographed with a Leica MPS40 camera, and processed with Adobe Photoshop software.

DNA analysis. Genomic DNA was analyzed by PCR using the primers p1, 5′-ATGCCCATACGGTTACTCTCA-3′, located in *Erf* intron 1; p2, 5′-AGAA GCACCCTTGAACACAGA-3′, located 3′ of *Erf* outside the targeting vector; and p3, 5′-ACAGCAGAGAAGAGAGAAGAG-3′, located in exon 4 (Fig. 1A). For Southern blots, genomic DNA was digested with EcoRI or BamHI and hybridized with probes derived from the 5′ (1.5-kb EcoRI/XbaI fragment) and the 3′ (0.6-kb PvuII fragment) flanking sequences or the internal 1-kb BamHI/SacI fragment (Fig. 1A).

RNA analysis. Total RNA was isolated using TRIzol reagent (Invitrogen) by following the manufacturer's instructions. For Northern analysis, 5 μg of RNA per lane was analyzed. The BamHI/SacI fragments from exon 4 of *Erf* (Fig. 1A), *Pl1* (7), *Eomes* (6), and *GAPDH* (18) were used as probes.

For quantitative PCR (QPCR), the RNA was treated with DNase (Ambion) reverse transcribed with superscript II and oligo(dT) primers (Invitrogen) and amplified with SYBR Green-containing kits (Stratagene and QIAGEN) on an Mx3000P instrument (Stratagene). In all cases the manufacturers' protocols were followed.

The following primers were used for cDNA amplification: *Cdx2*, TCTCCGA GAGGCAGGTTAAA/GCAAGGAGGTCACAGGACTC; *Eomes*, AAAGGT CGTTCAAGGTGCTG/GTTAACTCAAGGTCCAACCC; *Err*β, GGACACAC TGCTTTGAAGCA/ACAGATGTCTCTCATCTGGC; *Hand1*, ACCCTGACC CAGCCAAAGA/CAGGTACCGCTGTTGCTTG; *Mash2*, TGCGCTCCGCG GTAGAGTAC/TGCTTTCCTCCGACGAGTAGG; *Gcm1*, ACGAAGAGAT GGCATGCATG/CTTGTGACATTACACCTGGC; *Tpbp*, CGGAAGGCTCC AACATAGAA/TTTCGCTCGTTGCCTAACTT; *Pl1*, GGGCAGAAACCTTG TAATTC/ATGGATGTCCCTTTTAATGC; *Cph*, AGACCAGCAAGAAGAT CACC/GGAAAATATGGAACCCAAAG; *Gapdh*, CCAGTATGACTCCACT CACG/GACTCCACGACATACTCAGC; and *Erf*, CACCGAGATTCCTGAG AGC/AGAGACTAAAGAGAGCTGTCC and TACTCCAATGTACTCGGA GG/TGCACTTCAGGACACTACAG.

In situ hybridization. For in situ hybridization, frozen sections were postfixed in 4% paraformaldehyde in PBS for 10 min at room temperature (RT), washed twice in PBS, incubated in proteinase K for 5 min at 37°C, postfixed in 4% paraformaldehyde, washed in PBS, acetylated in 0.1 M triethanolamine–0.25% acetic anhydride for 10 min, and prehybridized for 2 h at 55°C in a hybridization solution containing 50% formamide, 5× SSC (1× SSC is 0.15 M NaCl plus 0.015 M sodium citrate), 5× Denhardt's solution, 0.25 mg/ml yeast RNA, and 0.5 mg/ml herring sperm DNA. Hybridization was performed overnight at 55°C in hybridization solution supplemented with 1 ng/μl of each digoxigenin-labeled riboprobe. After hybridization, the sections were washed in 2× SSC for 30 min at 55°C (twice), incubated in 20 μg/ml RNase for 30 min at 37°C, washed in 1× SSC for 30 min at 55°C, and incubated for 1 h at RT in 10% FCS. Sections were incubated overnight at 4°C with alkaline phosphatase (AP)-conjugated anti-digoxigenin (Roche), and the AP activity was detected with nitroblue tetrazolium/5-bromo-4-chloro-3-indolylphosphate.

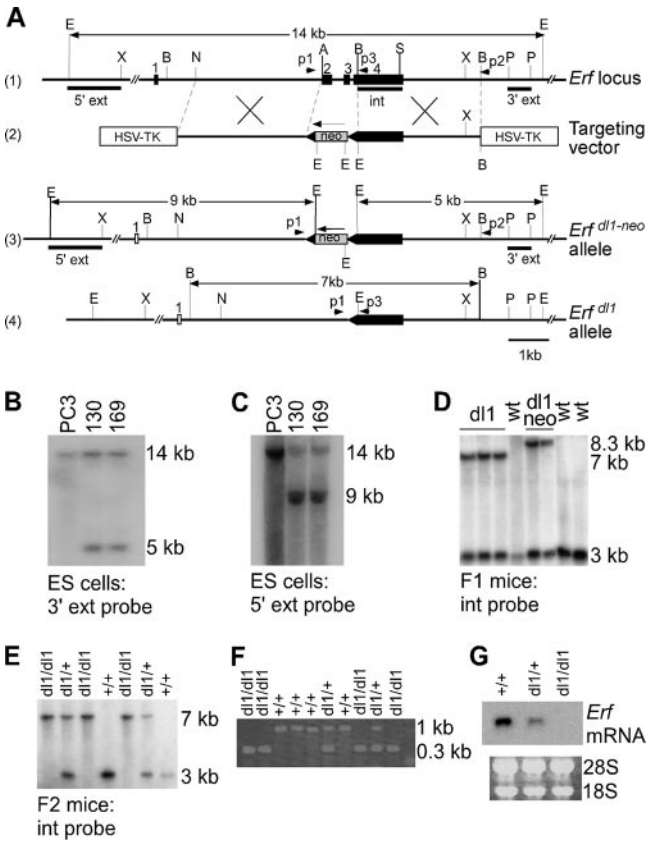

FIG. 1. Targeted disruption of the *Erf* gene. (A) Schematic representation of the Erf targeting strategy. (1) Genomic organization of the murine *Erf* gene. Exons are indicated by black boxes and are numbered 1 to 4. (2) The structure of the targeting vector. The AvrII-BamHI fragment was replaced by the pMC1neo cassette (gray box) flanked by loxP sites (black triangles). The arrow above indicates the orientation of the *neo* gene transcription. Dashed lines outline the *Erf* genomic sequences incorporated into the targeting construct. The herpes simplex virus thymidine kinase cassette (white box) was placed at both ends of the targeting vector for negative selection. (3) The predicted structure of the targeted *Erf* locus ($Erf^{dl1\text{-}neo}$) following homologous recombination of the targeting vector in ES cells. (4) The predicted structure of the targeted *Erf* locus (Erf^{dl1}) following Cre-mediated excision. Small arrows indicate the primers (p1, p2, and p3) used for genotyping by PCR. Boldface lines indicate the position of probes used for the Southern analysis. The sizes of the expected restriction fragments are also indicated. Restriction enzymes are the following: A, AvrII; B, BamHI; E, EcoRI; N, NotI; P, PvuII; S, SacI; X, XbaI. (B) Homologous recombination was verified by Southern analysis. Genomic DNA from control ES cells and two independently targeted ES clones, no. 130 and no. 169, was digested with EcoRI and hybridized to the radiolabeled 3′ external (3′ext) probe located outside of the targeting vector. The 14-kb fragment corresponding to the wild-type (wt) allele and the 5-kb fragment corresponding to the $Erf^{dl1\text{-}neo}$ allele are indicated. (C) Hybridization of genomic EcoRI fragments with the 5′ext probe. The 14-kb wild-type fragment and the 9-kb $Erf^{dl1\text{-}neo}$ fragment are indicated. (D) Southern blot analysis of genomic DNA from F_1 mice. DNA was digested with BamHI and hybridized to the radiolabeled internal (int) probe. Cre-recombined heterozygous mutant mice (dl1) were identified by the smaller 7-kb fragment, compared to the 8.3-kb mutant fragment of the nonrecombined allele (dl1-neo). The 3-kb band corresponds to the wild-type allele. (E) Southern blot analysis of genomic DNA derived from 9.5-dpc embryos of $Erf^{dl1/+}$ heterozygous mice intercross. The 3-kb band corresponds to the wild-type allele, and the 7-kb band corresponds to the Erf^{dl1} allele. (F) PCR analysis of genomic DNA derived from visceral yolk sacs of 9.5-dpc embryos from $Erf^{dl1/+}$ intercrosses using p1 and p3 primers. The wild-type allele is identified by the 1-kb band, and the Erf^{dl1} allele is identified by the 300-bp band. (G) Northern analysis of total RNA extracted from wild-type, heterozygous, and homozygous 9.5-dpc embryos, free of extraembryonic tissues, hybridized with the radiolabeled int probe (upper panel). Loading and integrity of RNA was assessed by ethidium bromide staining of the 28S and 18S rRNA in the gel (lower panel).

Both sense and antisense probes from the 1.1-kb BamHI/SacI fragment (exon 4) and a 1-kb SacI/XbaI fragment (3′ untranslated region) of *Erf* were prepared, and the presence of specific signal with the antisense *Erf* probes only was verified (see Fig. S1 in the supplemental material). Antisense RNA probes for *Pl1* (7), *Tpbpa* (37), *Err*β (40), *Gcm1* (4), and *Tef5* (28) have been described previously. The riboprobes were labeled with digoxigenin-11-UTP or fluorescein-12-UTP (Roche).

Protein analysis. Cryosections were air dried and fixed with methanol/acetone (1:1) for 10 min at −20°C. The sections were washed twice with PBS, blocked with 5% FCS, 3% bovine serum albumin for 30 min at RT, incubated overnight at 4°C with the 16-μg/ml CD106 rat monoclonal antibody (Pharmingen), washed, and incubated for 1 h at RT with anti-rat antibody–Alexa 555 (Molecular Probes). The sections were blocked consecutively with 5% normal rat serum and incubated overnight at 4°C with 25 μg/ml CD49d biotinylated rat monoclonal antibody (Pharmingen), washed, and incubated for 45 min at RT with dichlorotriazinylaminofluorescein)-conjugated streptavidin (Jackson). The nuclei were stained with To-Pro3 (Molecular Probes). Immunofluorescence analysis was performed using the TCS-NT laser scanning microscope (Leica) and analyzed with the Leica confocal software.

For immunoblotting, cell extracts were analyzed with an anti-Erk1/2 rabbit polyclonal antibody (Cell Signaling) or an anti-phospho-Erk1/2 monoclonal antibody (Sigma) and the corresponding secondary antibodies conjugated with horseradish peroxidase (Jackson). All antibodies were diluted in 25 mM Tris–150 mM NaCl–3 mM KCl–0.01% Tween 20.

RESULTS

Targeted disruption of the *Erf* gene in mice. To analyze the role of the *Erf* gene in vivo, we generated *Erf*-deficient mice by homologous recombination in ES cells. The *Erf*-targeting vector was designed to delete exons 2 and 3 and part of exon 4, encoding the ets DNA-binding domain, which is essential for the repressor activity of the protein (Fig. 1A) (56). The deleted genomic fragment also included five of the six splicing sites, minimizing the possibility of alternatively spliced products. This fragment was replaced with a loxP-flanked neomycin cassette to avoid potential transcriptional interference (16, 43) (Fig. 1A). The targeting vector was electroporated in PrmCre ES cells (42) that contain a Cre recombinase transgene under the control of the *Protamine-1* promoter, which is active in the male germ cells and results in the deletion of the loxP-flanked *neo* gene in F_1 mice. Six of the 179 tested G418- and ganciclovir-resistant clones were found by PCR to have undergone homologous recombination (data not shown). Genome integrity of homologous recombined clones was confirmed by Southern blot analysis using both the 3′ and 5′ regions external to the targeting vector probes (Fig. 1B and C) and chromosome count.

Two of the clones, no. 130 and no. 169, were injected into 3.5-dpc C57BL/6 blastocysts, and 20 chimeric mice were produced. Chimeric males derived from both clones were bred to C57BL/6 and 129/Sv wild-type females, and F_1 offspring with agouti coat color were analyzed for germ line transmission of the targeted *Erf* allele by Southern blotting (Fig. 1D). Eighty percent of the F_1 mice had undergone Cre-mediated recombination and were used in further experiments.

To ensure that we had generated a null mutation of the *Erf* gene, Northern blot analysis was performed on RNA isolated

TABLE 1. Genotype of 644 embryos and 240 F_2 mice from 114 $Erf^{dl1/+} \times Erf^{dl1/+}$ intercrosses of mixed C57BL/6 × 129/Sv or 129/Sv background[a]

Stage[b]	No. of litters	No. of embryos	No. (%) with genotype:			Comment
			+/+	*dl1*/+	*dl1*/*dl1*	
E8.5	10	79	20 (25)	41 (52)	18 (23)	
E9	4	30	7 (23)	14 (47)	9 (30)	
E9.5	42	376	82 (22)	179 (48)	116 (31)	
E10	5	42	8 (19)	23 (55)	11 (26)	
E10.5	10	89	19 (21)	47 (53)	23 (26)	22 of the $Erf^{dl1/dl1}$ embryos were dead
E11.5	3	28	8	17	3	5 Resorbtions
F_2	40	240	88 (37)	152 (63)	0	

[a] The viability status of the embryos was determined by their heartbeat at the moment of dissection.
[b] E8.5, embryonic day 8.5.

from 9.5-dpc independently genotyped embryos. The normal 2.8-kb *Erf* mRNA transcript was detected in the wild-type embryos and in a half dose in the heterozygous embryos but was absent in the homozygous embryos (Fig. 1G).

Analysis of *Erf* mutant mice. Heterozygous *Erf* mutant mice ($Erf^{dl1/+}$) in both genetic backgrounds (mixed C57BL/6 and 129/Sv) were normal and fertile and did not show any obvious phenotypic abnormality. However, genotyping of 240 live-born F_2 offspring obtained from 40 litters from heterozygous intercrosses failed to detect any viable homozygotes ($Erf^{dl1/dl1}$), indicating that the mutation is not transmitted in a Mendelian fashion and interferes with normal embryonic development (Table 1). $Erf^{dl1/+}$ and $Erf^{+/+}$ mice were recovered in a Mendelian ratio, as expected for a recessive embryonic-lethal mutation (Table 1). The genotypes of offspring from heterozygous intercrosses were determined by PCR and confirmed by Southern blot analysis (Fig. 1E).

To determine the time point at which $Erf^{dl1/dl1}$ embryos were dying, we analyzed the genotypes of embryos derived from heterozygous intercrosses at various stages of embryonic development. PCR analysis of postimplantation embryos dissected 8.5, 9.5, and 10.5 dpc showed that homozygotes were obtained with approximately Mendelian frequency (Fig. 1F; Table 1). Morphological examination of 10.5-dpc homozygous embryos showed that 22 (out of 23) embryos were dead, suggesting that Erf function is required for viability prior to this stage (Fig. 2A, panels c and d; Table 1). By 11.5 dpc, homozygote frequency deviated from the Mendelian ratio. Of 28 embryos analyzed at this stage, 3 $Erf^{dl1/dl1}$ embryos were in a highly degenerative state and 5 resorptions were observed, the genotype of which could not be determined (Table 1).

Analysis of *Erf* lethality. In order to identify the basis of embryonic lethality in $Erf^{dl1/dl1}$ embryos, we performed morphological and histological analysis of embryos and extraembryonic tissues at stages 8.5 and 9.5 dpc. By 8.5 dpc $Erf^{dl1/dl1}$ embryos were normal compared with their control littermates. In contrast, by 9.5 dpc 17 out of 21 $Erf^{dl1/dl1}$ embryos were smaller in size and weight than their control littermates, though they were in the same developmental stage as determined by somite number (Fig. 2A, panels a and b). These embryos also showed defects in the head region, with forebrain, midbrain, and hindbrain hypoplasia. In a smaller number (10%) of $Erf^{dl1/dl1}$ embryos a highly congestive edema bilateral to the head was observed (see Fig. S2 in the supplemental material). Also, 7% of the $Erf^{dl1/dl1}$ embryos had not completed the closure of the neural tube. In other structures, like the branchial arches, otic vesicles, eye primordia, anterior limb bud, and heart, we did not notice any apparent abnormalities in $Erf^{dl1/dl1}$ embryos. However, all the $Erf^{dl1/dl1}$ embryos already exhibited extensive apoptosis at 9.5 dpc, indicative of their detrimental fate (see Fig. S9 in the supplemental material). A few nondegenerated embryos at 10.5 dpc were dead and anemic (Fig. 2A, panels c and d).

It is unlikely that the embryonic abnormalities could account for the $Erf^{dl1/dl1}$ embryo lethality. Embryonic lethality at midgestation often is the result of failure to establish and maintain a vascular circulation between the mother and the fetus, including those mediated by the yolk sac and the chorioallantoic placenta (8). The mouse yolk sac sustains maternal and fetal nutrient exchange until 9.5 dpc. Also, the yolk sac is the site of primary hematopoiesis and blood vessel formation from clusters of blood islands that, during vasculogenesis, fuse to form a primitive capillary plexus followed by angiogenesis (48, 49). Whole-mount examination of 9.5-dpc yolk sacs revealed that the large vitelline vessels are formed in the wild type and heterozygotes (Fig. 2B, panel a), whereas only a primary vascular network was visible in $Erf^{dl1/dl1}$ yolk sacs (Fig. 2B, panel b). Also, in contrast to the wild type and heterozygotes, $Erf^{dl1/dl1}$ yolk sacs appeared pale. Whole-mount staining with hematoxylin indicated that the collecting vessels formed, but they were larger and failed to form secondary branches and a well-organized vascular network (Fig. 2B, panels c and d). Histological analysis of cross-sections of 9.5-dpc yolk sacs showed that disruption of *Erf* function did not prevent blood island formation containing primitive nucleated red blood cells (see Fig. S3 in the supplemental material). Histological examination of sections of 9.5-dpc embryos indicated that circulation between yolk sac and embryo proper vasculature had not been disrupted. The viability of $Erf^{dl1/dl1}$ embryos up to 10 dpc suggested that the observed yolk sac abnormalities could not account for the embryonic lethality but may reflect a hypoxia/stress-induced phenotype.

***Erf*$^{dl1/dl1}$ embryos have severe placenta abnormalities.** The mortality in $Erf^{dl1/dl1}$ embryos observed after 10 dpc coincides with the establishment of chorioallantoic circulation. Histological analysis of $Erf^{dl1/dl1}$ placentas showed severe defects in their development and morphogenesis compared to the wild-type and heterozygote littermates. In wild-type placentas chorioallantoic attachment had been completed by 8.5 dpc, followed by folding of the chorionic plate (Fig. 2C, panel a). In $Erf^{dl1/dl1}$ placentas, the allantois had reached the chorion and appeared to make contact but failed to attach. The chorion remained intact and retained its compact structure, characteristic of earlier stages (Fig. 2C, panel b). The ectoplacental cone cavity that is normally closed by 8.0 dpc persisted and became wider in later stages. In contrast to the wild type, $Erf^{dl1/dl1}$ placentas also exhibited a smaller spongiotrophoblast layer.

At 9.5 dpc, in wild-type placentas (Fig. 2C, panels c and c′) allantoic mesoderm and underlying fetal blood vessels interdigitated with chorion trophoblast cells, and simple branches were formed that elongated and bifurcated to establish the labyrinthine layer. In $Erf^{dl1/dl1}$ placentas (Fig. 2C, panels d and d′), the chorioallantoic interface did not form and the chorion

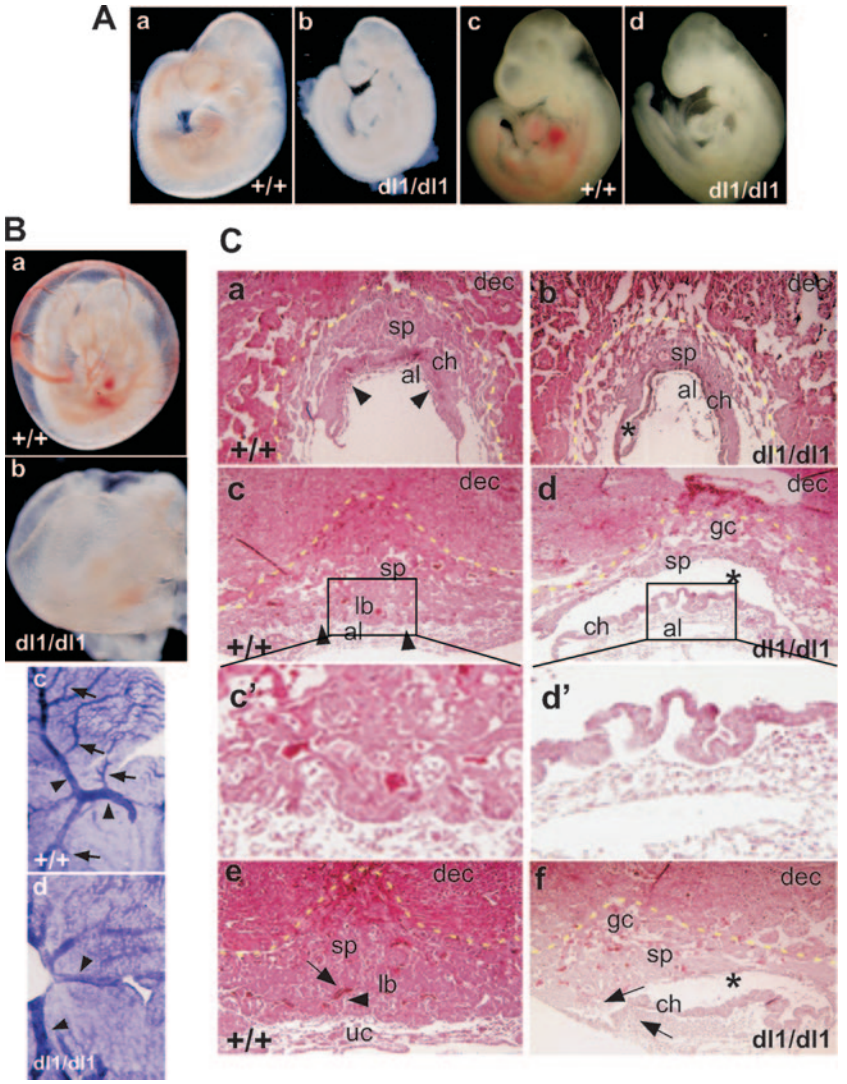

FIG. 2. Phenotype of the *Erf*-deficient mouse embryos. (A) Gross morphology of 9.5-dpc wild-type (a) and $Erf^{dl1/dl1}$ (b) embryos and 10.5-dpc wild-type (c) and $Erf^{dl1/dl1}$ (d) embryos. (B) Yolk sac morphology of a wild-type (a) and an $Erf^{dl1/dl1}$ (b) embryo at 9.5 dpc. A highly organized vascular network is formed in wild-type yolk sacs, whereas in $Erf^{dl1/dl1}$ embryos the yolk sacs are pale and exhibit only the primary capillary plexus without further reorganization. Whole-mount staining of wild-type (c) and $Erf^{dl1/dl1}$ (d) yolk sacs with hematoxylin are also shown. Large collecting vessels are formed in both wild-type and $Erf^{dl1/dl1}$ yolk sacs (arrowheads), but in $Erf^{dl1/dl1}$ they are enlarged and do not form secondary branches (arrows) as in the wild-type littermates. (C) Hematoxylin- and eosin-stained paraffin sections from wild-type (a, c, c′, and e) and $Erf^{dl1/dl1}$ (b, d, d′, and f) littermates. At 8.5 dpc the allantois is attached throughout the chorion layer in the wild-type placentas (panel a, arrowheads) but not in $Erf^{dl1/dl1}$ placentas, where the ectoplacemmtal cone cavity is still open (panel b, asterisk). At 9.5 dpc allantoic blood vessels invade the chorion layer in wild-type placentas (arrowheads in panels c, c′), but in the $Erf^{dl1/dl1}$ placentas the chorion retains a compact structure, the labyrinth is totally absent (d′), and the ectoplacental cone cavity is still present (panel d, asterisk). At 10.5 dpc in wild-type placentas, maternal and embryonic blood vessels (panel e, arrow and arrowhead, respectively) intermingle and come to close apposition. In contrast, $Erf^{dl1/dl1}$ placentas appear degenerative, with extensive hemorrhagic sites (panel f, arrows). al, allantois; ch, chorion; dec, decidua; gc, giant cells; lb, labyrinth; sp, spongiotrophoblast; uc, umbilical cord. Yellow dotted lines indicate the boundaries of the placenta.

of the $Erf^{dl1/dl1}$ placentas retained a compact structure. In addition, the ectoplacental cone cavity remained open, and spongiotrophoblast and giant cell layers were severely disorganized. $Erf^{dl1/dl1}$ placentas also exhibited a decreased spongiotrophoblast and an expanded giant cell layer (see Fig. S4 in the supplemental material).

By 10.5 dpc in wild-type placentas, maternal sinuses and embryonic blood vessels intermingled and came into close proximity (Fig. 2C, panel e), umbilical cord vessels were formed from the allantoic blood vessels, and chorioallantoic circulation was evident. In contrast, $Erf^{dl1/dl1}$ placentas (Fig. 2C, panel f) maintained the same morphology as in the earlier stage. Also, in $Erf^{dl1/dl1}$ placentas the umbilical cord did not form from allantoic vessels, which appeared collapsed. In addition, $Erf^{dl1/dl1}$ placentas exhibited extensive hemorrhage-forming pools of blood in both the ectoplacental cone cavity and the allantoic compartment.

These data strongly suggest that the embryonic mortality of $Erf^{dl1/dl1}$ embryos is due to their failure to establish a functional chorioallantoic circulation.

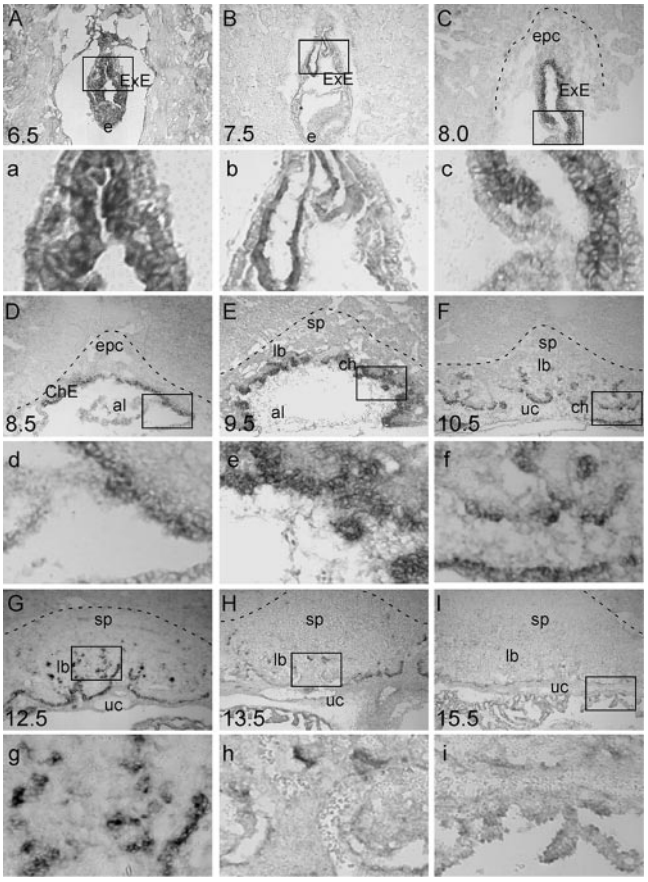

FIG. 3. Expression of *Erf* in the developing placenta. In situ hybridization of *Erf* mRNA in sagittal sections of wild-type placentas from 6.5 to 15.5 dpc using a 1-kb riboprobe derived from *Erf* exon 4. (A to C) Through early placenta development (6.5 to 8.0 dpc) *Erf* mRNA is detected in the ExE. (D) At 8.5 dpc *Erf* mRNA is detected throughout the chorionic ectoderm (ChE). (E) By 9.5 dpc *Erf* mRNA persists in the chorion (ch). It is also detected in some trophoblast cells in the developing labyrinth. (F and G) At 10.5 to 12.5 dpc *Erf* transcripts are present in the chorion and in the labyrinthine trophoblast cells. (H and I) At 13.5 dpc *Erf* mRNA expression in the chorion and in labyrinthine trophoblasts is decreased and disappears after 15.5 dpc. (a to i) Magnification of the indicated areas (boxes) of panels A through I. al, allantois; e, embryo; epc, ectoplacental cone; lb, labyrinth; sp, spongiotrophoblast; uc, umbilical cord. Dotted lines indicate the boundaries of the placenta.

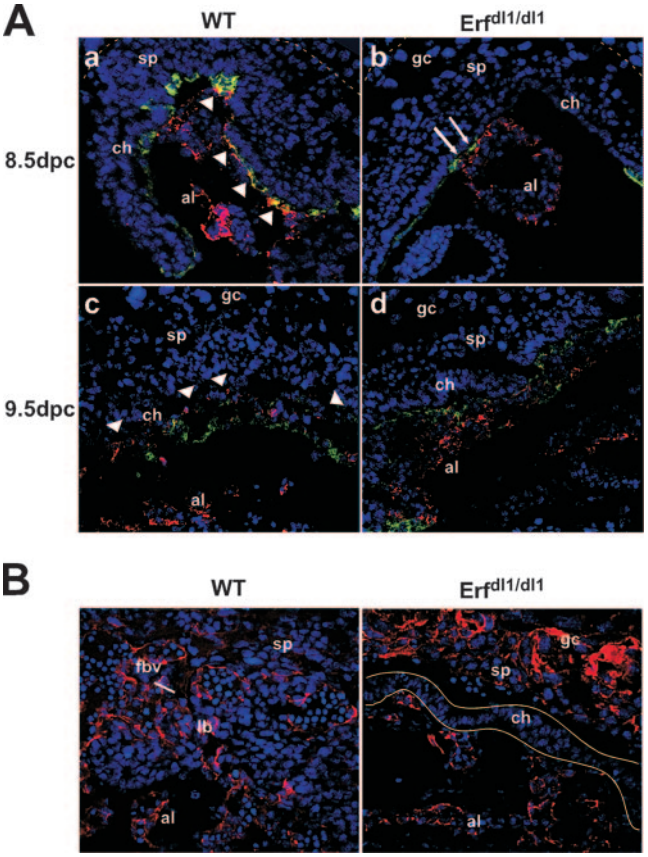

FIG. 4. Failure of chorioallantoic attachment in $Erf^{dl1/dl1}$ embryos. (A) Confocal microscopy images from sagittal sections of 8.5-dpc (a and b) and 9.5-dpc (c and d) placentas. Freshly frozen placentas were stained with antibodies against the allantoic protein VCAM-1 (red) and the chorionic protein integrin α4 (green). Nuclei were stained with TOPRO-3 (blue). (a) In 8.5-dpc wild-type (WT) placentas, attachment of allantoic mesothelium with chorionic mesoderm throughout the chorion layer is evidenced by the yellow color (arrowheads). (b) Both VCAM1 and integrin α4 are expressed in $Erf^{dl1/dl1}$ placentas. The mesothelial surface of allantois approaches the chorionic mesoderm (arrows) but fails to fuse and spread throughout the chorionic layer. (c) In 9.5-dpc wild-type placentas, chorioallantoic fusing surfaces break down, enabling the juxtaposition of allantoic vasculature and chorion layer, resulting in the penetration of allantoic endothelium to the chorion, indicated by the VCAM1 staining at both sides of the chorion layer (arrowheads). (d) In $Erf^{dl1/dl1}$ placentas, the proximity of allantois can be seen throughout the chorionic mesoderm, but there is no penetration of allantoic mesothelium or even contact of the two layers, as indicated by the lack of yellow color. Yellow dotted lines indicate the boundaries of the placenta. (B) PECAM staining (red) in wild-type and $Erf^{dl1/dl1}$ placentas from 9.5 dpc. Nuclei were stained blue with TOPRO-3. The yellow lines in the right panel indicate the chorion layer in $Erf^{dl1/dl1}$ placentas. al, alantois; lb, labyrinth; ch, chorion; sp, spongoid layer; gc, giant cells; fbv, fetal blood vessels.

***Erf* exhibits a distinct pattern of expression in the developing placenta.** To determine if the chorion-specific phenotype of *Erf* is associated with the expression of the gene, we analyzed its expression in both embryonic and extraembryonic tissues. In the developing placenta, *Erf* expression was examined from the onset of gastrulation at 6.5 dpc to 15.5 dpc of fetal development. In contrast to its ubiquitous expression in the embryo and adult (data not shown), *Erf* exhibited a very restrictive pattern in the developing placenta. By 6.5 to 7.5 dpc, *Erf* mRNA could be detected in the ExE (Fig. 3A, a, B, and b). At 8.0 dpc its expression was restricted in the ExE and the ExE derivative (Fig. 3C and c). At 8.5 dpc it could be detected throughout the chorionic ectoderm (Fig. 3D and d), and at 9.5 dpc it could be detected throughout the diploid chorion trophoblast cell layer and some of the labyrinthine trophoblasts (Fig. 3E and e) but not in differentiated cells expressing *Gcm1* (see Fig. S5 in the supplemental material). During 10.5 to 12.5 dpc, a more restricted pattern of *Erf* expression was detected in the chorion trophoblast cells and labyrinthine trophoblast cells (Fig. 3F, f, G, and g). Expression at these sites decreased at 13.5 dpc and ceased after 15.5 dpc (Fig. 3H, h, I, and i).

Interestingly, *Erf* transcripts were not detected in the ectoplacental cone or its derivative, the spongiotrophoblast layer,

or in giant cell layer. In contrast to the placenta, *Erf* expression could be detected at low levels throughout the embryo proper, in the endoderm of the yolk sac, and in allantois.

The *Erf* expression pattern would be consistent with the embryonic and extraembryonic defects noticed in $Erf^{dl1/dl1}$ embryos and would suggest a role in chorion cell regulation.

Failure of chorioallantoic attachment. To further elucidate the apparent failure of the chorioallantoic attachment observed by histological analysis in $Erf^{dl1/dl1}$ placentas, we performed immunohistochemical staining for VCAM1 and its counterreceptor integrin α4, both found in genetic studies to play indispensable roles during chorioallantoic attachment. VCAM1 is expressed by the mesothelial cells of the allantois, while integrin α4 is expressed by the chorionic mesoderm, a cell layer that lines the chorionic ectoderm (24, 33, 70). Immunostaining of sections from 8.5- and 9.5-dpc placentas revealed that the disruption of *Erf* does not affect VCAM1 and integrin α4 expression, and both molecules were expressed from the respective cell types in $Erf^{dl1/dl1}$ conceptuses (Fig. 4A). In wild-type placentas, the allantois attached to the entire surface of the chorionic plate by 8.5 dpc (yellow staining in Fig. 4A, panel a). In contrast, in $Erf^{dl1/dl1}$ placentas, despite the proximity of chorion and allantois, colocalization of VCAM1 and integrin α4 could not be detected (Fig. 4A, panel b). The possibility of a chorioallantoic attachment delay in $Erf^{dl1/dl1}$ placentas was assessed at 9.5 dpc. Although allantois had spread across the chorion, attachment was not evident (as determined by yellow color) and spaces between the chorion and allantois were present (Fig. 4A, panel d). In contrast, in wild-type placentas by 9.5 dpc chorioallantoic attachment sites had been broken down and allantoic vasculature had penetrated to the chorion, as shown by the detection of VCAM1 both at the chorion layer and at the allantoic compartment (Fig. 4A, panel c) (13). In $Erf^{dl1/dl1}$ placentas, the allantoic mesoderm differentiated into vascular structures, as evidenced by the expression of PECAM, but did not penetrate the chorion as occurred in the wild-type placentas (Fig. 4B).

These data suggest that *Erf* is required for chorioallantoic attachment, though it does not appear to directly affect the formation of the cell types mediating this interaction.

***Erf* function is necessary for chorionic trophoblast cell differentiation.** Placenta abnormalities observed during histological analysis were further characterized by RNA in situ hybridization and the expression of specific markers for different placenta cell types. The giant cell layer, as assessed by the expression of *Pl1* (placental lactogen-1), which marks the secondary giant cells, was not affected at 8.5 dpc (Fig. 5A, panels a and e). In contrast, the giant cell layer was significantly expanded in $Erf^{dl1/dl1}$ placentas at both 9.5 (Fig. 5B, panels a, a′, e, and e′) and 10.5 (Fig. 5C, panels a and e) dpc compared with wild-type placentas. The spongiotrophoblast cell layer, as assessed by the expression of *Tpbpa*, was greatly reduced in $Erf^{dl1/dl1}$ placentas at 8.5 dpc (Fig. 5A, panels b and f), 9.5 dpc (Fig. 5B, panels b, b′, f, and f′), and 10.5 dpc (Fig. 5C, panels b and f). In order to determine if the reduced size of the spongiotrophoblast layer was due to impaired cell proliferation, we examined the incorporation of 5-bromo-2′-deoxyuridine into DNA in spongiotrophoblast cells. We found that there was not a significant difference in cell proliferation of spongiotrophoblast cells between $Erf^{dl1/dl1}$ and wild-type placentas (see Fig. S6 in the supplemental material). The labyrinth formation in $Erf^{dl1/dl1}$ placentas was assessed by the expression of *Tef5*, which is normally expressed in chorion trophoblast cells and from syncytiotrophoblasts (28). *Tef5* expression was undetectable in 9.5-dpc (Fig. 5B, panels d, d′, h, and h′) and 10.5-dpc (Fig. 5C, panels d and h) $Erf^{dl1/dl1}$ placentas, consistent with the absence of the labyrinth.

To determine if the absence of labyrinth formation and the persistence of a compact chorion layer in $Erf^{dl1/dl1}$ placentas were related to possible differentiation defects, we assessed the expression of trophoblast markers for these layers. Expression of *Err*β, a marker for trophoblast stem cells, extraembryonic ectoderm, and chorionic ectoderm (40) was elevated in $Erf^{dl1/dl1}$ placentas. In wild-type placentas at 8.5 dpc, *Err*β was detected only in the free margins of the chorion, whereas in $Erf^{dl1/dl1}$ placentas it could be detected throughout the chorionic ectoderm (Fig. 5A, panels d and h) and persisted until 9.0 dpc (data not shown), suggesting a delayed differentiation of chorion trophoblast cells.

We further assessed the defects in ExE differentiation and labyrinth formation by *Gcm1* expression. *Gcm1*, which is normally expressed in a subset of chorion trophoblast cells where chorioallantoic folding will start at 8.5 dpc (1), is totally absent from $Erf^{dl1/dl1}$ placentas (Fig. 5A, panels c and g). By 9.5 dpc *Gcm1* was expressed from syncytiotrophoblast cells of the forming labyrinth and arrested chorion trophoblast cells in wild-type placentas, but it could not be detected in $Erf^{dl1/dl1}$ placentas (Fig. 5B, panels c, c′, g, and g′). It was also absent from 10.5-dpc $Erf^{dl1/dl1}$ placentas (Fig. 5C, panels c and g), consistent with the lack of chorioallantoic attachment and labyrinth development.

To determine if the lack of labyrinth is a result of the lack of chorioallantoic attachment or defective chorion cell differentiation, we examined *Gcm1* expression at 8.0 dpc, before chorioallantoic attachment. In wild-type placentas speckled *Gcm1* expression, suggestive of the chorion patterning (10), was evident. In contrast, in $Erf^{dl1/dl1}$ placentas *Err*β was evident throughout the chorion, but we were unable to detect any *Gcm1* expression (Fig. 6).

The prolonged expression of *Err*β and the absence of *Gcm1* suggest that the defect in ExE differentiation precedes chorioallantoic attachment and may be responsible for the $Erf^{dl1/dl1}$ phenotype.

***Erf* affects TSC differentiation.** To determine if the changes in differentiation of various placental cell layers were due to cell-autonomous defects in the trophoblast lineage, we studied the phenotype of $Erf^{dl1/dl1}$ trophoblast stem cell lines derived from wild-type and $Erf^{dl1/dl1}$ blastocysts and examined the expression of *Erf* and lineage-specific markers during differentiation. *Erf* was expressed in proliferating wild-type TSCs, and its expression was initially increased during differentiation and decreased when the cells were terminally differentiated to giant cells (Fig. 7A and B). Interestingly, *Erf* expression was increased while Erk activity was decreased (Fig. 7C), suggesting not only higher Erf levels but higher levels of transcriptionally active nuclear Erf that could alter the transcription program of these cells. In the absence of *Erf*, TSCs could differentiate in vitro towards giant cells, similar to the wild-type cells (see Fig. S7 and S8 in the supplemental material). However, in contrast to the wild-type TSCs, all four $Erf^{dl1/dl1}$ TSC lines

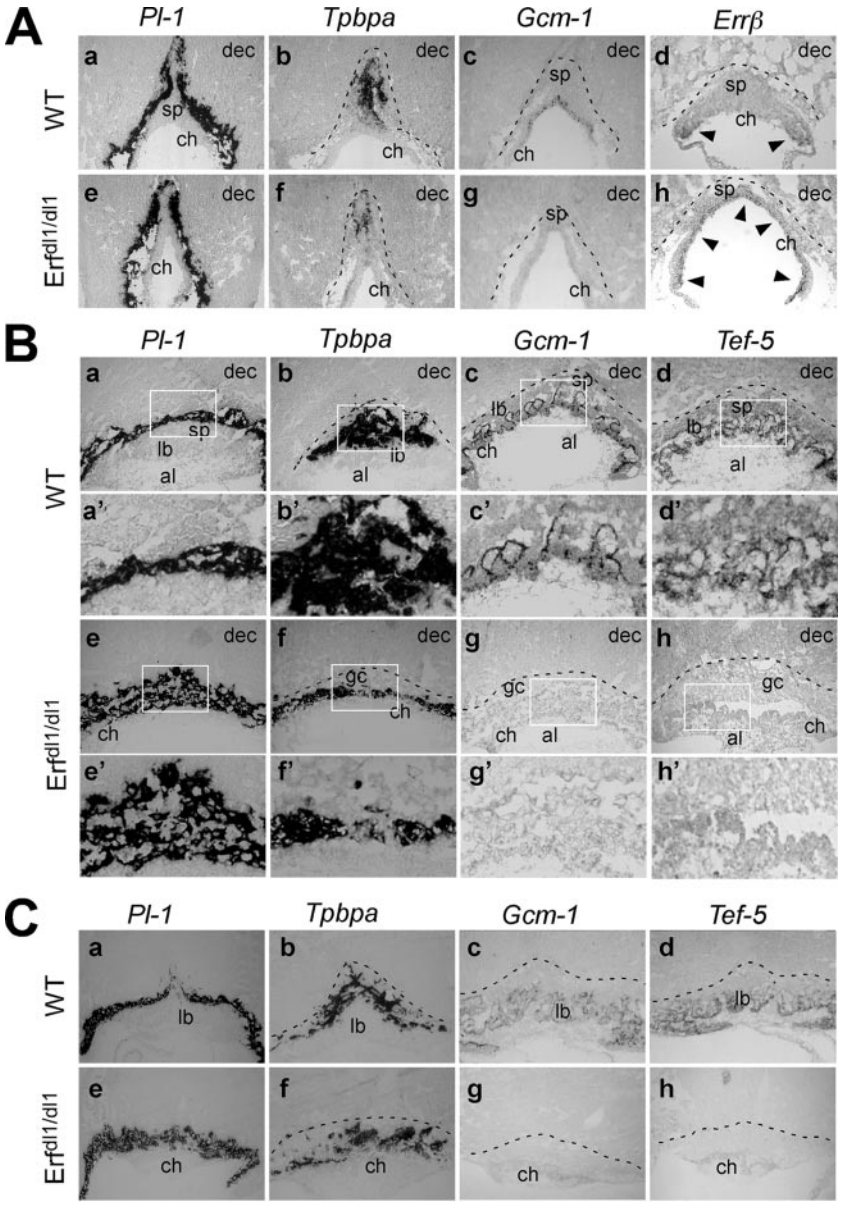

FIG. 5. Expression of cell type-specific markers in the developing placenta. (A) In situ hybridization was performed on frozen sections from 8.5-dpc wild-type (WT) (a to d) and $Erf^{dl1/dl1}$ (e to h) placentas with antisense RNA probes for *Pl1*, *Tpbpa*, *Gcm1*, and *Err*β. Expression of *Pl1* is unaffected in $Erf^{dl1/dl1}$ placentas (a and e). Expression of *Tpbpa* is reduced in $Erf^{dl1/dl1}$ placentas (b and f). *Gcm1*, which is expressed in a subset of chorionic trophoblast cells in wild-type placentas, is absent from $Erf^{dl1/dl1}$ placentas (c and g). *Err*β is expressed (arrowheads) at the margins of the chorion in wild-type placentas, while in $Erf^{dl1/dl1}$ placentas (h) it is detected throughout the chorion (d and h). (B) In situ hybridization on sections from 9.5-dpc wild-type (a to d) and $Erf^{dl1/dl1}$ (e to h) placentas with probes for *Pl1*, *Tpbpa*, *Gcm1*, and *Tef5.* Expression of *Pl1* in $Erf^{dl1/dl1}$ placentas reveals an expansion of trophoblast giant cell layer (e and e′). Expression of *Tpbpa* shows a reduced spongiotrophoblast cell layer in $Erf^{dl1/dl1}$ placentas (f and f′). *Gcm1* is expressed in syncytiotrophoblasts of the labyrinthine layer and in chorionic trophoblast cells in wild-type placentas (c and c′) but is not detectable in $Erf^{dl1/dl1}$ placentas (g and g′). *Tef5* is expressed in syncytiotrophoblasts and in labyrinthine trophoblasts in wild-type placentas (d and d′) but is not present in $Erf^{dl1/dl1}$ placentas (h and h′). (a′ to h′) Magnification of the indicated regions (white rectangles) from panels a through h, respectively. (C) In situ hybridization on sections from 10.5-dpc placentas as described for panel B. The giant cell layer remains expanded (a and e), the trophoblast cell layer is disorganized (b and f), and the sycytiotrophoblast cells (c, g, d, and h) are missing in $Erf^{dl1/dl1}$ animals. dec, decidual; al, allantois; lb, labyrinth; sp, spongiotrophoblasts; gc, giant cells. Dotted lines indicate the boundaries of the placenta.

analyzed exhibited a delayed differentiation, as evidenced by the 10- to 20-fold higher levels of the TSC-specific markers *Cdx2*, *Eomes*, and *Err*β 2 to 4 days after growth factor withdrawal (Fig. 7D and E). The other striking finding was that the expression of the spongiotrophoblast-specific marker *Tpbpa* in $Erf^{dl1/dl1}$ TSCs was 15- to 100-fold lower than that of the wild-type TSCs (Fig. 7F). TS cells do not differentiate towards syncytiotrophoblasts in vitro; thus, the role of Erf in this branch could not be determined. However, the delayed differentiation and the near absence of spongiotrophoblast cells support our in vivo findings and suggest that *Erf*, in addition to its paramount role in chorion cell

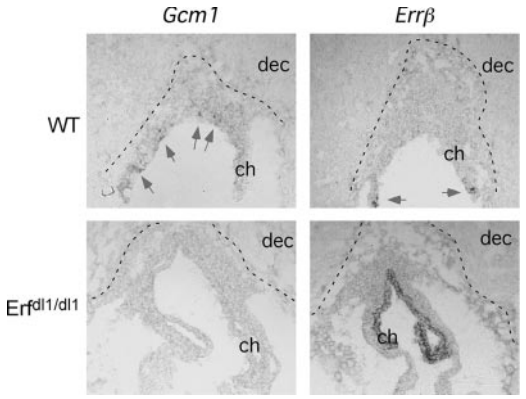

FIG. 6. *Gcm1* expression in the developing placenta at 8.0 dpc. In situ hybridization was performed on frozen sections from 8.0-dpc wild-type (upper panel) and $Erf^{dl1/dl1}$ (lower panel) placentas with *Gcm1* (left panels) and *Err*β (right panels) antisense RNA probes. The arrows indicate points of *Gcm1* expression. dec, decidual; ch, chorion; WT, wild type. Dotted lines indicate the boundaries of the placenta.

differentiation, may be necessary for the balanced TSC lineage commitment.

DISCUSSION

ets family genes share a common DNA binding domain that recognizes a purine-rich sequence and have been implicated in a number of biological processes, most commonly the reproductive and the immune systems as well as in tumorigenesis. The overlapping expression pattern of these genes (27) makes the determination of the biological function of specific ets domain genes difficult.

In order to elucidate the function of *Erf*, a ubiquitously expressed ets domain gene with transcriptional repressor activity that is regulated by Erks, we generated mice with a targeted *Erf* deletion that inactivates the gene. $Erf^{dl1/dl1}$ animals are embryonic lethal due to severe placenta defects. Our data indicate that $Erf^{dl1/dl1}$ embryos fail to complete chorion cell differentiation and undergo chorioallantoic attachment.

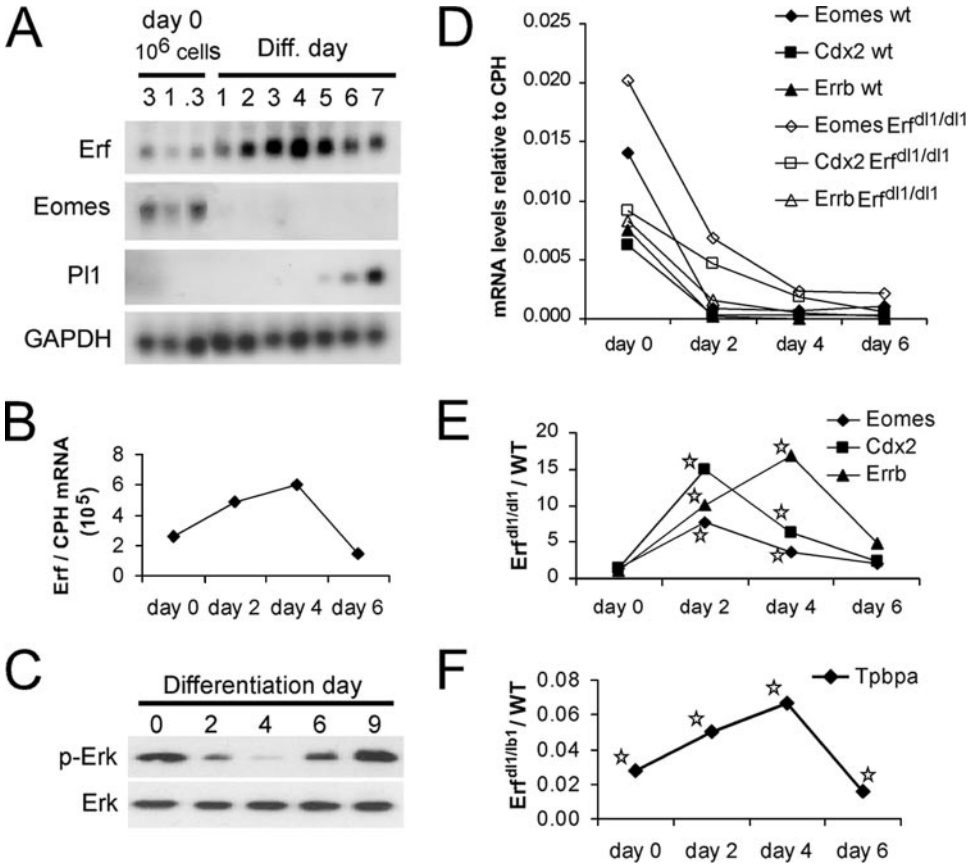

FIG. 7. Gene expression in differentiating TSCs. (A) RNA from wild-type (WT) TSC under proliferation conditions at the indicated cell densities (day 0) and the indicated times (differentiation [Diff.] day) in differentiation media was analyzed by Northern blotting for the expression of *Erf*, the TSC marker *Eomes*, the giant cell marker *Pl1*, and *GAPDH* as a loading control. (B) The level of *Erf* mRNA during TSC differentiation was determined by QPCR and compared to the *Cph* mRNA levels in the same sample. The average of two independent wild-type cell lines is shown. (C) Protein extracts from differentiating wild-type TSCs were analyzed by immunoblotting to determine the levels of total (upper panel) and activated (lower panel) Erks. (D) The mRNA levels of *Eomes*, *Cdx2*, and *Err*β from wild-type (filled symbols) and $Erf^{dl1/dl1}$ (open symbols) TSCs were analyzed by QPCR and are presented as fractions of the *Cph* mRNA value in each sample. The graph presents the average of four $Erf^{dl1/dl1}$ cell lines and two wild-type cell lines. (E) The values of the $Erf^{dl1/dl1}$ samples from panel D were divided by the corresponding values of the wild-type samples to determine differences in TSC marker expression. (F) As described for panel E, the average values of the *Tpbpa* levels from the four $Erf^{dl1/dl1}$ and the two wild-type TSC cell lines were divided to determine the differential expression of *Tpbpa* during TSC differentiation. Stars in panels E and F indicate statistically significant differences, with *P* values between 0.01 and 0.05.

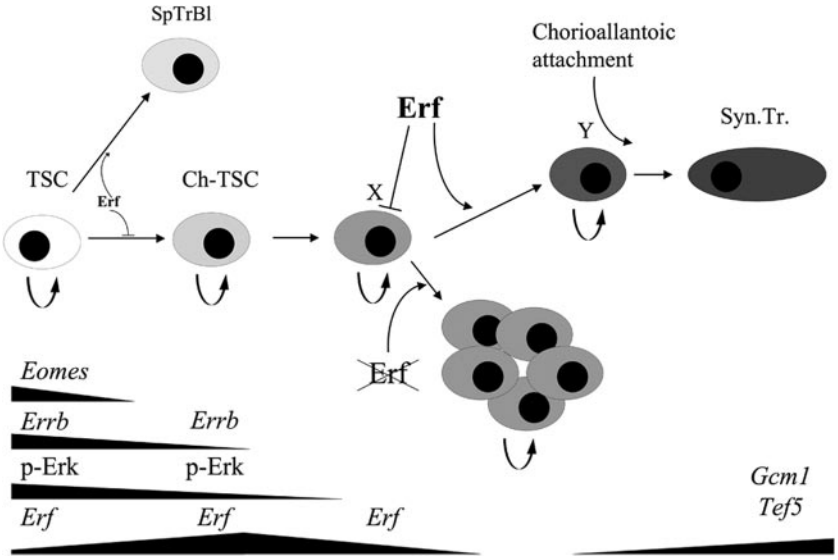

FIG. 8. Model for the role of *Erf* in TSC differentiation. *Erf* may affect the proper initial commitment of TSCs. At a later stage elevated levels of Erf in the absence of Erk activity are required for the differentiation of chorion diploid cells to terminally differentiated syncytiotrophoblasts (Syn.Tr.), ectoplacental cone cavity closure, and chorioallantic attachment. Ch-TSC, chorion TSC.

They therefore fail to form the labyrinth layer of the placenta, which is the layer critical by midgestation for nutrient exchange between the maternal and fetal circulation. In addition, they fail to close the ectoplacental cone cavity and have an expanded giant cell layer and a diminished spongiotrophoblast layer, while quite often they are hemorrhagic. Thus, although other causes cannot be absolutely excluded, failed placentation appears to be the reason for embryonic death.

Analysis of $Erf^{dl1/dl1}$ trophoblast stem cells in conjunction with the expression pattern of *Erf* and the Erk activity in the developing placenta (9) suggests that *Erf* may have a dual role in the differentiation of TSCs (Fig. 8). The kinetics of $Erf^{dl1/dl1}$ TSC differentiation, the prolonged expression of the ExE marker *Err*β in $Erf^{dl1/dl1}$ placentas, and the defects in specific placenta layers that do not express detectable levels of *Erf* suggest that Erf may be important for regulating the timing and/or balance of TSC differentiation. This is consistent with a role as a downstream FGF/Erk effector, the major TSC-regulating pathway.

Erf appears to be absolutely required for the differentiation of the chorion trophoblast cells. By 7.5 dpc *Erf* is expressed specifically in these cells at a time when the Erk activity is absent (9), facilitating its nuclear accumulation and function. Thus, *Erf* may define a new intermediate in trophoblast differentiation that does not express any of the stem cell markers (*Cdx2*, *Eomes*, and *Err*β) or terminal differentiation markers (*Gcm1* and *Tef5*). In the absence of *Erf* these cells fail to properly differentiate, as suggested by the absence of *Gcm1* and persistence of *Err*β expression, and they continue to proliferate (see Fig. S6 in the supplemental material), suggesting that nuclear *Erf* may actively promote chorionic trophoblast differentiation.

The most striking characteristic of the *Erf* absence is the total failure of the chorioallantoic attachment. Chorioallantoic attachment is the first necessary step in labyrinth morphogenesis (11), and key interacting proteins such as VCAM1 and integrin α4 are required for the proper contact of the allantois with the chorion, interdigitation, and the development of the labyrinth. Erf is expressed in both the allantois and the chorion at this time, and its loss could be affecting either or both sites. In the $Erf^{dl1/dl1}$ embryos both structures appear normal by 8.5 dpc, they express VCAM1 and integrin α4, and they are in close proximity. However, we could not detect colocalization of VCAM1 and integrin α4 or the consecutive interdigitation that is found in the wild-type placentas. The molecular mechanism by which Erf affects chorioallantoic attachment is not clear at this point. TGFβ and Wnt signaling are known to affect this process (30, 44, 64). However, the allantois, the chorionic mesoderm, and the expression of specific proteins, such as VCAM1, integrin α4, Flk1, and PECAM, appear normal in $Erf^{dl1/dl1}$ embryos, suggesting that Erf may not directly interfere with these structures.

A unique characteristic of the $Erf^{dl1/dl1}$ placentas is the apparent failure to close the ectoplacental cone cavity, a step required in placenta development (66). Expansion of the basal ectoplacental cone layer and the ExE layer leads to the closure of the cavity. *Erf* is the only gene that appears to affect this process thus far. The diminished spongiotrophoblast layer in $Erf^{dl1/dl1}$ placentas as well as the dramatically decreased expression of *Tpbpa* during $Erf^{dl1/dl1}$ TSC differentiation suggests that ectoplacental cone-derived cells may be responsible for this defect, supporting the hypothesis that *Erf* may affect proper commitment of TSCs. Although the specific ExE cell population that contributes to the ectoplacental cone cavity closure is not currently identifiable, the expression of *Erf* in the ExE and the chorion suggests that it may also be expressed in these cells. Thus, it is plausible that the $Erf^{dl1/dl1}$ defect in ExE differentiation may also affect the chorionic contribution in the closure of the cavity. The absence of Erk activity from the chorion and its presence in the ectoplacental cone at this stage (9) indicate that loss of Erf, which would reproduce some aspects of persisting FGF signaling, is more likely to affect the

ExE contribution in the cavity closure. The expanded cavity between the chorion and spongiotrophoblast layer, usually observed around 9.5 dpc, that quite often leads to placenta disruption could be a secondary event resulting from the maternal blood concentration that fails to circulate properly due to the lack of labyrinth development.

A final defect in the $Erf^{dl1/dl1}$ placentas is the decreased spongiotrophoblast layer and the expanded giant cell layer. We could not detect *Erf* expression in either of these layers. Thus, these abnormalities may result either from the defects of the chorion layer or from a defect in TSC commitment during differentiation. Both cases have been reported in the past. Loss of the *Lpl* (19) or the *Esx1* (38) gene affects these two layers, though these genes are not expressed in the spongiotrophoblast and the giant cell layers. However, a more plausible hypothesis is the defective differentiation of a common ectoplacental cone precursor, as suggested by Simmons and Cross and supported by the phenotype of genes like *Mash2* (23), *Chorioderemia* (58), and *Keratin 8/19* (61) that have opposing effects in these two cell layers. Our data on the delayed in vitro differentiation of the TSC lines as well as the dramatically low levels of spongiotrophoblast marker *Tpbpa* suggest that Erf may indeed affect the differentiation of a common precursor. The state of FGF/Erk signaling is not known in this hypothetical common precursor; thus, the mechanism of Erf function cannot be deciphered at this stage. We examined the proliferation (see Fig. S6 in the supplemental material) and apoptosis (see Fig. S9 in the supplemental material) rates in $Erf^{dl1/dl1}$ placentas to determine if the observed changes are the results of altered proliferation or death. Our data indicate that they cannot account for the decreased spongiotrophoblast layer and the increased giant cell layer. Although marginal *Erf* expression in these two layers cannot be excluded, our data support the hypothesis of a common precursor, the differentiation of which is affected by *Erf*.

Our hypothesis about the function of *Erf* in the developing placenta is that it mediates lack of FGF signals. In $Erf^{dl1/dl1}$ animals the attenuation of FGF4/Erk signaling, normally observed by 7.5 dpc in the chorion (9), that would allow Erf nuclear localization and function is disrupted. The absence of nuclear Erf is perceived as the presence of mitogenic signal that blocks ExE differentiation, and immature cells still occupy the chorion (Fig. 8). These cells fail to contribute to ectoplacental cone cavity closure. Signals from these cells or lack of required signals from the now absent, more differentiated chorion cells block chorioallantoic attachment and result in the halt of the whole process. In either case, our data suggest that chorion trophoblast cell differentiation is a prerequisite for chorioallantoic attachment.

FGF signaling has been shown to be a major pathway in TSC proliferation and differentiation. In addition, the FGF pathway plays an important role in ExE differentiation and labyrinth development (68). Many key components of the pathway, such as *Grb2* (54), *Sos* (46), *B-Raf* (20), and *Mek1* (21), exhibit defects in labyrinth development, mostly in proper branching and angiogenesis. However, at the time of labyrinth development the Erk activity is undetectable in this layer (9), suggesting either that prior commitment of the cells is necessary for proper differentiation or that Erk-dependent signals from other areas of the developing embryo are required for proper labyrinth development. In either case defects in the Erk activation pathway should not reproduce the $Erf^{dl1/dl1}$ phenotype, since they should result in Erf nuclear accumulation and transcriptional repression rather than loss of Erf function. On the other hand, it is unclear if *Erf* is contributing to the labyrinth phenotype of FGF pathway mutants, since $Erf^{dl1/dl1}$ placentas do not reach the branching stage. However, our data strongly suggest that the elimination of Erk activity from the ExE that would allow Erf to enter the nucleus and exert its transcriptional control is also required for placenta development. This would be an additional indication that proper temporal and special Erk activity is paramount for placenta development and suggest that attenuation of FGF signaling is also important in placenta development.

In addition to the placental defects, the yolk sac appears to have some anomalies. Although the role of Erks in angiogenesis is established, it is not clear if the defects observed in yolk sac arteries are related to Erk signaling (32, 71). As mentioned above, loss-of-function mutations in the Erk pathway cannot be recapitulated by *Erf* loss. However, in the absence of animals with constitutive active Erk, we cannot exclude at this point an angiogenic effect of *Erf* within the Erk signaling pathway. It is common, though, for placental defects to result in apparent yolk sac anomalies around 9.5 dpc as a consequence of the attempt to compensate for the lack of chorioallantoic circulation and the resulting hypoxia and stress (see Fig. S10 in the supplemental material). Thus, the increased number of blood islands and size of main arteries could be the result of the need for additional nutrients. The increased number of blood islands could also disrupt the apparent secondary vein network of the yolk sac. Such changes in the yolk sac have also been observed in some *Gcm1* mutant conceptuses as well (J. Cross, unpublished observations).

The apparent defects in the embryo proper, as in the case of the decreased size, may also be due to the lack of labyrinth development. It is a common side effect of the placental defects, a result of malnutrition of the embryo as evidenced by the dramatic elevation of Hif1a expression (see Fig. S10 in the supplemental material). Placental defects are usually associated with cardiovascular defects in the embryo proper. However, in the case of 9.5-dpc $Erf^{dl1/dl1}$ embryos the cardiovascular system appears unaffected (see Fig. S11 in the supplemental material). It is unclear at this point if *Erf* loss results in additional defects in the embryo proper. Given the ubiquitous expression of the gene and its regulation by a major signaling pathway, this should not be excluded. Additional experiments are required to address this issue.

In conclusion, our data indicate that *Erf* is required for chorion cell differentiation and suggest that chorion differentiation is a prerequisite for chorioallantoic attachment. They also indicate that it has a role in trophoblast stem cell balance in lineage commitment and support the hypothesis of a common precursor for giant and trophoblast cell layers. They support the dominant role of the FGF/Erk signaling pathway in placenta development and suggest that its attenuation is required for chorion differentiation. Finally, they provide evidence that *Erf* may be the first gene identified to affect ectoplacental cone cavity closure and suggest that specific differentiation steps are required for this process, rather than simple spatial expansion of the adjacent layers.

ACKNOWLEDGMENTS

We are grateful to the IMBB animal facility personnel for keeping of the mice, S. O'Gorman of Case Western Reserve University for the PC3 ES cells, G. Kollias of the BSRC "Alexander Fleming" for his support, Ling Wang of the BIMR Mouse Molecular Genetics Shared Resource for blastocyst isolation, and Laura Virgilio for helpful discussions.

This work was supported by EU grant HPRN-CT-2000-00083, PYTHAGORAS II grant KA2091, and GSRT grant PENED99 to G.M. and in part by RO1CA098778, PO1CA102583, and Cancer Center Support Grant CA 30199 from the National Cancer Institute.

REFERENCES

1. **Anson-Cartwright, L., K. Dawson, D. Holmyard, S. J. Fisher, R. A. Lazzarini, and J. C. Cross.** 2000. The glial cells missing-1 protein is essential for branching morphogenesis in the chorioallantoic placenta. Nat. Genet. **25:** 311–314.
2. **Arman, E., R. Haffner-Krausz, Y. Chen, J. K. Heath, and P. Lonai.** 1998. Targeted disruption of fibroblast growth factor (FGF) receptor 2 suggests a role for FGF signaling in pregastrulation mammalian development. Proc. Natl. Acad. Sci. USA **95:**5082–5087.
3. **Bartel, F. O., T. Higuchi, and D. D. Spyropoulos.** 2000. Mouse models in the study of the Ets family of transcription factors. Oncogene **19:**6443–6454.
4. **Basyuk, E., J. C. Cross, J. Corbin, H. Nakayama, P. Hunter, B. Nait-Oumesmar, and R. A. Lazzarini.** 1999. Murine Gcm1 gene is expressed in a subset of placental trophoblast cells. Dev. Dyn. **214:**303–311.
5. **Chen, C., W. Ouyang, V. Grigura, Q. Zhou, K. Carnes, H. Lim, G. Q. Zhao, S. Arber, N. Kurpios, T. L. Murphy, A. M. Cheng, J. A. Hassell, V. Chandrashekar, M. C. Hofmann, R. A. Hess, and K. M. Murphy.** 2005. ERM is required for transcriptional control of the spermatogonial stem cell niche. Nature **436:**1030–1034.
6. **Ciruna, B. G., and J. Rossant.** 1999. Expression of the T-box gene Eomesodermin during early mouse development. Mech. Dev. **81:**199–203.
7. **Colosi, P., J. J. Swiergiel, E. L. Wilder, A. Oviedo, and D. I. Linzer.** 1988. Characterization of proliferin-related protein. Mol. Endocrinol. **2:**579–586.
8. **Copp, A. J.** 1995. Death before birth: clues from gene knockouts and mutations. Trends Genet. **11:**87–93.
9. **Corson, L. B., Y. Yamanaka, K. M. Lai, and J. Rossant.** 2003. Spatial and temporal patterns of ERK signaling during mouse embryogenesis. Development **130:**4527–4537.
10. **Cross, J. C., H. Nakano, D. R. Natale, D. G. Simmons, and E. D. Watson.** 2006. Branching morphogenesis during development of placental villi. Differentiation **74:**393–401.
11. **Cross, J. C., D. G. Simmons, and E. D. Watson.** 2003. Chorioallantoic morphogenesis and formation of the placental villous tree. Ann. N. Y. Acad. Sci. **995:**84–93.
12. **Donnison, M., A. Beaton, H. W. Davey, R. Broadhurst, P. L'Huillier, and P. L. Pfeffer.** 2005. Loss of the extraembryonic ectoderm in Elf5 mutants leads to defects in embryonic patterning. Development **132:**2299–2308.
13. **Downs, K. M.** 2002. Early placental ontogeny in the mouse. Placenta **23:** 116–131.
14. **Erlebacher, A., K. A. Price, and L. H. Glimcher.** 2004. Maintenance of mouse trophoblast stem cell proliferation by TGF-beta/activin. Dev. Biol. **275:**158–169.
15. **Feldman, B., W. Poueymirou, V. E. Papaioannou, T. M. DeChiara, and M. Goldfarb.** 1995. Requirement of FGF-4 for postimplantation mouse development. Science **267:**246–249.
16. **Fiering, S., E. Epner, K. Robinson, Y. Zhuang, A. Telling, M. Hu, D. I. Martin, T. Enver, T. J. Ley, and M. Groudine.** 1995. Targeted deletion of 5′HS2 of the murine beta-globin LCR reveals that it is not essential for proper regulation of the beta-globin locus. Genes Dev. **9:**2203–2213.
17. **Firulli, A. B., D. G. McFadden, Q. Lin, D. Srivastava, and E. N. Olson.** 1998. Heart and extra-embryonic mesodermal defects in mouse embryos lacking the bHLH transcription factor Hand1. Nat. Genet. **18:**266–270.
18. **Fort, P., L. Marty, M. Piechaczyk, S. el Sabrouty, C. Dani, P. Jeanteur, and J. M. Blanchard.** 1985. Various rat adult tissues express only one major mRNA species from the glyceraldehyde-3-phosphate-dehydrogenase multigenic family. Nucleic Acids Res. **13:**1431–1442.
19. **Frank, D., W. Fortino, L. Clark, R. Musalo, W. Wang, A. Saxena, C. M. Li, W. Reik, T. Ludwig, and B. Tycko.** 2002. Placental overgrowth in mice lacking the imprinted gene Ipl. Proc. Natl. Acad. Sci. USA **99:**7490–7495.
20. **Galabova-Kovacs, G., D. Matzen, D. Piazzolla, K. Meissl, T. Plyushch, A. P. Chen, A. Silva, and M. Baccarini.** 2006. Essential role of B-Raf in ERK activation during extraembryonic development. Proc. Natl. Acad. Sci. USA **103:**1325–1330.
21. **Giroux, S., M. Tremblay, D. Bernard, J. F. Cardin-Girard, S. Aubry, L. Larouche, S. Rousseau, J. Huot, J. Landry, L. Jeannotte, and J. Charron.** 1999. Embryonic death of Mek1-deficient mice reveals a role for this kinase in angiogenesis in the labyrinthine region of the placenta. Curr. Biol. **9:**369–372.
22. **Gu, H., J. D. Marth, P. C. Orban, H. Mossmann, and K. Rajewsky.** 1994. Deletion of a DNA polymerase beta gene segment in T cells using cell type-specific gene targeting. Science **265:**103–106.
23. **Guillemot, F., T. Caspary, S. M. Tilghman, N. G. Copeland, D. J. Gilbert, N. A. Jenkins, D. J. Anderson, A. L. Joyner, J. Rossant, and A. Nagy.** 1995. Genomic imprinting of Mash2, a mouse gene required for trophoblast development. Nat. Genet. **9:**235–242.
24. **Gurtner, G. C., V. Davis, H. Li, M. J. McCoy, A. Sharpe, and M. I. Cybulsky.** 1995. Targeted disruption of the murine VCAM1 gene: essential role of VCAM-1 in chorioallantoic fusion and placentation. Genes Dev. **9:**1–14.
25. **Guzman-Ayala, M., N. Ben-Haim, S. Beck, and D. B. Constam.** 2004. Nodal protein processing and fibroblast growth factor 4 synergize to maintain a trophoblast stem cell microenvironment. Proc. Natl. Acad. Sci. USA **101:** 15656–15660.
26. **Hogan, B.** 1994. Manipulating the mouse embryo: a laboratory manual. Cold Spring Harbor Laboratory Press, Plainview, NY.
27. **Hollenhorst, P. C., D. A. Jones, and B. J. Graves.** 2004. Expression profiles frame the promoter specificity dilemma of the ETS family of transcription factors. Nucleic Acids Res. **32:**5693–5702.
28. **Jacquemin, P., V. Sapin, E. Alsat, D. Evain-Brion, P. Dolle, and I. Davidson.** 1998. Differential expression of the TEF family of transcription factors in the murine placenta and during differentiation of primary human trophoblasts in vitro. Dev. Dyn. **212:**423–436.
29. **Janknecht, R.** 2005. EWS-ETS oncoproteins: the linchpins of Ewing tumors. Gene **363:**1–14.
30. **Jones, R. L., C. Stoikos, J. K. Findlay, and L. A. Salamonsen.** 2006. TGF-β superfamily expression and actions in the endometrium and placenta. Reproduction **132:**217–232.
31. **Kaufman, M. H.** 1992. The atlas of mouse development. Academic Press, London, United Kingdom.
32. **Kuida, K., and D. M. Boucher.** 2004. Functions of MAP kinases: insights from gene-targeting studies. J. Biochem. (Tokyo) **135:**653–656.
33. **Kwee, L., H. S. Baldwin, H. M. Shen, C. L. Stewart, C. Buck, C. A. Buck, and M. A. Labow.** 1995. Defective development of the embryonic and extraembryonic circulatory systems in vascular cell adhesion molecule (VCAM-1) deficient mice. Development **121:**489–503.
34. **Laing, M. A., S. Coonrod, B. T. Hinton, J. W. Downie, R. Tozer, M. A. Rudnicki, and J. A. Hassell.** 2000. Male sexual dysfunction in mice bearing targeted mutant alleles of the PEA3 ets gene. Mol. Cell. Biol. **20:**9337–9345.
35. **Le Gallic, L., D. Sgouras, G. Beal, Jr., and G. Mavrothalassitis.** 1999. Transcriptional repressor ERF is a Ras/mitogen-activated protein kinase target that regulates cellular proliferation. Mol. Cell. Biol. **19:**4121–4133.
36. **Le Gallic, L., L. Virgilio, P. Cohen, B. Biteau, and G. Mavrothalassitis.** 2004. ERF nuclear shuttling, a continuous monitor of Erk activity that links it to cell cycle progression. Mol. Cell. Biol. **24:**1206–1218.
37. **Lescisin, K. R., S. Varmuza, and J. Rossant.** 1988. Isolation and characterization of a novel trophoblast-specific cDNA in the mouse. Genes Dev. **2:**1639–1646.
38. **Li, Y., and R. R. Behringer.** 1998. Esx1 is an X-chromosome-imprinted regulator of placental development and fetal growth. Nat. Genet. **20:**309–311.
39. **Liu, D., E. Pavlopoulos, W. Modi, N. Moschonas, and G. Mavrothalassitis.** 1997. ERF: genomic organization, chromosomal localization and promoter analysis of the human and mouse genes. Oncogene **14:**1445–1451.
40. **Luo, J., R. Sladek, J. A. Bader, A. Matthyssen, J. Rossant, and V. Giguere.** 1997. Placental abnormalities in mouse embryos lacking the orphan nuclear receptor ERR-beta. Nature **388:**778–782.
41. **Meissner, A., and R. Jaenisch.** 2006. Generation of nuclear transfer-derived pluripotent ES cells from cloned Cdx2-deficient blastocysts. Nature **439:**212–215.
42. **O'Gorman, S., N. A. Dagenais, M. Qian, and Y. Marchuk.** 1997. Protamine-Cre recombinase transgenes efficiently recombine target sequences in the male germ line of mice, but not in embryonic stem cells. Proc. Natl. Acad. Sci. USA **94:**14602–14607.
43. **Olson, E. N., H. H. Arnold, P. W. Rigby, and B. J. Wold.** 1996. Know your neighbors: three phenotypes in null mutants of the myogenic bHLH gene MRF4. Cell **85:**1–4.
44. **Parr, B. A., V. A. Cornish, M. I. Cybulsky, and A. P. McMahon.** 2001. Wnt7b regulates placental development in mice. Dev. Biol. **237:**324–332.
45. **Polychronopoulos, S., M. Verykokakis, M. N. Yazicioglu, M. Sakarellos-Daitsiotis, M. H. Cobb, and G. Mavrothalassitis.** 2006. The transcriptional repressor ETS2 factor associates with active and inactive Erks through distinct FXF motifs. J. Biol. Chem. **281:**25601–25611.
46. **Qian, X., L. Esteban, W. C. Vass, C. Upadhyaya, A. G. Papageorge, K. Yienger, J. M. Ward, D. R. Lowy, and E. Santos.** 2000. The Sos1 and Sos2 Ras-specific exchange factors: differences in placental expression and signaling properties. EMBO J. **19:**642–654.
47. **Riley, P., L. Anson-Cartwright, and J. C. Cross.** 1998. The Hand1 bHLH transcription factor is essential for placentation and cardiac morphogenesis. Nat. Genet. **18:**271–275.
48. **Risau, W.** 1997. Mechanisms of angiogenesis. Nature **386:**671–674.

49. **Risau, W., and I. Flamme.** 1995. Vasculogenesis. Annu. Rev. Cell Dev. Biol. **11:**73–91.
50. **Ristevski, S., D. A. O'Leary, A. P. Thornell, M. J. Owen, I. Kola, and P. J. Hertzog.** 2004. The ETS transcription factor GABPalpha is essential for early embryogenesis. Mol. Cell. Biol. **24:**5844–5849.
51. **Rossant, J., and J. C. Cross.** 2001. Placental development: lessons from mouse mutants. Nat. Rev. Genet. **2:**538–548.
52. **Rothenberg, E. V., and T. Taghon.** 2005. Molecular genetics of T cell development. Annu. Rev. Immunol. **23:**601–649.
53. **Russ, A. P., S. Wattler, W. H. Colledge, S. A. Aparicio, M. B. Carlton, J. J. Pearce, S. C. Barton, M. A. Surani, K. Ryan, M. C. Nehls, V. Wilson, and M. J. Evans.** 2000. Eomesodermin is required for mouse trophoblast development and mesoderm formation. Nature **404:**95–99.
54. **Saxton, T. M., A. M. Cheng, S. H. Ong, Y. Lu, R. Sakai, J. C. Cross, and T. Pawson.** 2001. Gene dosage-dependent functions for phosphotyrosine-Grb2 signaling during mammalian tissue morphogenesis. Curr. Biol. **11:**662–670.
55. **Seth, A., and D. K. Watson.** 2005. ETS transcription factors and their emerging roles in human cancer. Eur. J. Cancer **41:**2462–2478.
56. **Sgouras, D. N., M. A. Athanasiou, G. J. Beal, Jr., R. J. Fisher, D. G. Blair, and G. J. Mavrothalassitis.** 1995. ERF: an ETS domain protein with strong transcriptional repressor activity, can suppress ets-associated tumorigenesis and is regulated by phosphorylation during cell cycle and mitogenic stimulation. EMBO J. **14:**4781–4793.
57. **Sharrocks, A. D.** 2001. The ETS-domain transcription factor family. Nat. Rev. Mol. Cell Biol. **2:**827–837.
58. **Shi, W., J. A. van den Hurk, V. Alamo-Bethencourt, W. Mayer, H. J. Winkens, H. H. Ropers, F. P. Cremers, and R. Fundele.** 2004. Choroideremia gene product affects trophoblast development and vascularization in mouse extra-embryonic tissues. Dev. Biol. **272:**53–65.
59. **Simmons, D. G., and J. C. Cross.** 2005. Determinants of trophoblast lineage and cell subtype specification in the mouse placenta. Dev. Biol. **284:**12–24.
60. **Spyropoulos, D. D., P. N. Pharr, K. R. Lavenburg, P. Jackers, T. S. Papas, M. Ogawa, and D. K. Watson.** 2000. Hemorrhage, impaired hematopoiesis, and lethality in mouse embryos carrying a targeted disruption of the Fli1 transcription factor. Mol. Cell. Biol. **20:**5643–5652.
61. **Tamai, Y., T. Ishikawa, M. R. Bosl, M. Mori, M. Nozaki, H. Baribault, R. G. Oshima, and M. M. Taketo.** 2000. Cytokeratins 8 and 19 in the mouse placental development. J. Cell Biol. **151:**563–572.
62. **Tanaka, S., T. Kunath, A. K. Hadjantonakis, A. Nagy, and J. Rossant.** 1998. Promotion of trophoblast stem cell proliferation by FGF4. Science **282:**2072–2075.
63. **Tootle, T. L., and I. Rebay.** 2005. Post-translational modifications influence transcription factor activity: a view from the ETS superfamily. Bioessays **27:**285–298.
64. **Tremblay, K. D., N. R. Dunn, and E. J. Robertson.** 2001. Mouse embryos lacking Smad1 signals display defects in extra-embryonic tissues and germ cell formation. Development **128:**3609–3621.
65. **Tsang, M., and I. B. Dawid.** 2004. Promotion and attenuation of FGF signaling through the Ras-MAPK pathway. Sci. STKE **2004:**pe17.
66. **Uy, G. D., K. M. Downs, and R. L. Gardner.** 2002. Inhibition of trophoblast stem cell potential in chorionic ectoderm coincides with occlusion of the ectoplacental cavity in the mouse. Development **129:**3913–3924.
67. **Wang, L. C., F. Kuo, Y. Fujiwara, D. G. Gilliland, T. R. Golub, and S. H. Orkin.** 1997. Yolk sac angiogenic defect and intra-embryonic apoptosis in mice lacking the Ets-related factor TEL. EMBO J. **16:**4374–4383.
68. **Xu, X., M. Weinstein, C. Li, M. Naski, R. I. Cohen, D. M. Ornitz, P. Leder, and C. Deng.** 1998. Fibroblast growth factor receptor 2 (FGFR2)-mediated reciprocal regulation loop between FGF8 and FGF10 is essential for limb induction. Development **125:**753–765.
69. **Yamamoto, H., M. L. Flannery, S. Kupriyanov, J. Pearce, S. R. McKercher, G. W. Henkel, R. A. Maki, Z. Werb, and R. G. Oshima.** 1998. Defective trophoblast function in mice with a targeted mutation of Ets2. Genes Dev. **12:**1315–1326.
70. **Yang, J. T., H. Rayburn, and R. O. Hynes.** 1995. Cell adhesion events mediated by alpha 4 integrins are essential in placental and cardiac development. Development **121:**549–560.
71. **Zachary, I.** 2003. VEGF signalling: integration and multi-tasking in endothelial cell biology. Biochem. Soc. Trans. **31:**1171–1177.